Sheet-like assemblies of spherical particles with point-symmetrical patches

Ethayaraja Mani,[1,a),b)] Eduardo Sanz,[2,c)] Soumyajit Roy,[1,d)] Marjolein Dijkstra,[2] Jan Groenewold,[1] and Willem K. Kegel[1,a)]
[1]*Van' t Hoff Laboratory for Physical and Colloid Chemistry, Debye Institute, Utrecht University, Padualaan 8, 3584 CH Utrecht, The Netherlands*
[2]*Soft Condensed Matter Group, Debye Institute, Utrecht University, Princetonplein 5, 3584 CC Utrecht, The Netherlands*

(Received 15 December 2011; accepted 22 March 2012; published online 11 April 2012)

We report a computational study on the spontaneous self-assembly of spherical particles into two-dimensional crystals. The experimental observation of such structures stabilized by spherical objects appeared paradoxical so far. We implement patchy interactions with the patches point-symmetrically (icosahedral and cubic) arranged on the surface of the particle. In these conditions, preference for self-assembly into sheet-like structures is observed. We explain our findings in terms of the inherent symmetry of the patches and the competition between binding energy and vibrational entropy. The simulation results explain why hollow spherical shells observed in some Keplerate-type polyoxometalates (POM) appear. Our results also provide an explanation for the experimentally observed layer-by-layer growth of apoferritin - a quasi-spherical protein. © *2012 American Institute of Physics*. [http://dx.doi.org/10.1063/1.3702203]

I. INTRODUCTION

Spontaneous assembly of monomers into two-dimensional structures has been observed for a variety of objects ranging from colloidal rods[1] to surfactants/lipids[2] and semiconductor nanocrystals.[3] The formation of bilayers and liquid-crystal phases by surfactants/lipids are related to their rod-like shape and amphiphilicity.[2] Similarly, a truncated tetragonal shape in addition to dipolar and hydrophobic interactions are responsible for the formation of sheet-like structure by CdTe nanocrystals.[3] The intrinsic abilities to form two-dimensional structures in these cases are then attributed to either anisotropic shape or directional interactions of the monomers.

Significantly more puzzling are the experimental observations of the formation of two-dimensional crystals in two widely different, yet quasi-spherical objects. These objects are certain Keplerate-type polyoxometalates (POM[4]) and the protein apoferritin.[5] The Keplerates are quasi-spherical hollow icosidodecahedral structures built by molybdenum-based oxides,[6] and further details of the structure is discussed below. Inspired by these observations, we address the question: under what conditions do the seemingly spherical particles stabilize two-dimensional crystals? A simulation study demonstrated that only when attractive binding sites (patches) are distributed along the equatorial plane, these particles self assemble into an expected two-dimensional crystal.[7] Here, as an important difference, we consider spherical particles with attractive patches distributed according to certain point-symmetries such that they are compatible to build space-filling three-dimensional crystals. Intuitively, it is expected that these patchy particles self-assemble into a crystal. Yet, we observe self-assembly into two-dimensional crystals. POMs are known to self-assemble into large hollow shell-like structures (20–50 nm diameter) under certain conditions.[4,8] We address the formation of 2D structures by spherical particles in general without explicitly addressing shells. It is then anticipated that the sheet-like 2D structures eventually grow and fold into shells.

We study two types of spherical patchy models: a 30-patch model with patches at the icosidodecahedral dispositions (Fig. 1(b)) and a 24-patch model that has a pair of patches on the 12 faces of the rhombododecahedron (Fig. 1(d)). The 30- patch model has the icosahedral symmetry (I_h) with C2, C3, and C5 symmetry axes, while the 24-patch model has cubic symmetry (F432) with C2, C3, and C4 symmetry axes.

The patchy models resemble structurally well-defined and naturally occurring inorganic POM molecules[9] of diameter 2.5 nm, and apoferritin protein[10] of diameter 10 nm. The 30-patch model corresponds to the spherical Keplerate-type POMs of general formula $\{Mo_{72}X_{30}\}$, where X is either a mononuclear transition metal such as Fe, V, Cr, or binuclear linker like $\{Mo_2\}$. A set of 12 pentagonal $\{(Mo)Mo_5\}$ molybdenum oxide units form the basic icosahedron, which are connected by 30 linkers (X), giving rise to a quasi-spherical shape known as Keplerate, as shown in Fig. 1(a).[9] The dispositions of X span the vertices of a regular icosidodecahedron. Water molecules bound to the linkers can form hydrogen bonds with other POMs.[11] The 24-patch model resembles the structure of apoferritin, which has 24 asymmetric units assembled in pairs (antiparallel) on the 12 faces of a quasi-rhombododecahedron

a)Authors to whom correspondence should be addressed. Electronic addresses: ethaya@iitm.ac.in and w.k.kegel@uu.nl. Tel: +91 44 2257 4157 and +31 30 253 2873. Fax: +91 44 2257 4152 and +31 30 253 3870.
b)Present address: Department of Chemical Engineering, Indian Institute of Technology Madras, Chennai 600036, India.
c)Present address: Departamento de Quimica Fisica I, Facultad de Ciencias Quimicas, Universidad Complutense, 28040 Madrid, Spain.
d)Present address: Chemical Sciences, Indian Institute of Science Education and Research, Kolkata 700064, India.

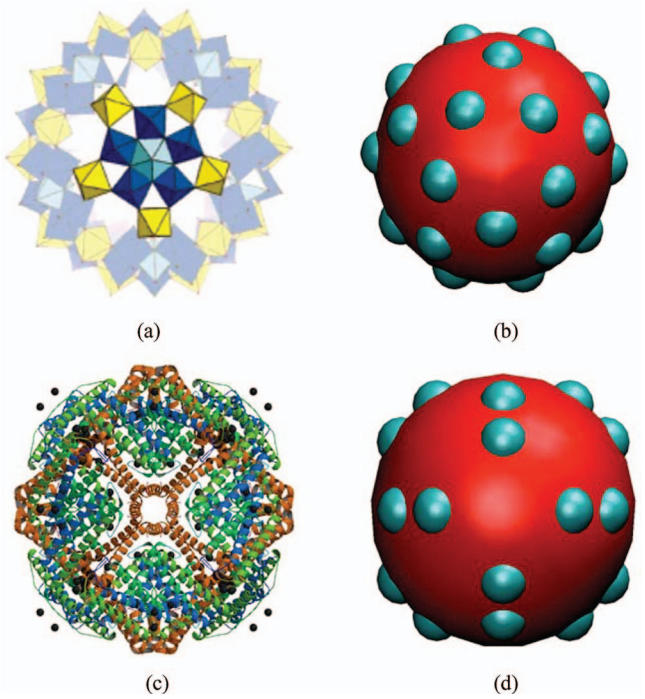

FIG. 1. (a) An example of Keplerate POM $\{Mo_{72}X_{30}\}$, where 12 pentagonal $\{(Mo)Mo_5\}$ fragments (shown in light and dark blue color) assemble in an icosahedron, which are in turn connected by 30 linker (X) molecules (shown in yellow) to give rise to a quasi-spherical icosidodecahedron (Refs. 6 and 9). One of the pentagonal units and its linkers are highlighted. (b) An equivalent 30-patch model for POM. (c) Crystal structure of apoferritin protein (Ref. 10) and (d) an equivalent 24-patch model.

(Fig. 1(c)). On each unit, there are two metal (Cd) binding residues (Asp 84 and Gln 86). Due to the antiparallel arrangement of the units, these residues (Asp-Gln) cooperatively form two metal binding sites along the longer diagonal of the face. Therefore two divalent metals are sandwiched between a pair of apoferritin particles.[10] The hydrogen bonding sites in POMs and metal binding sites in apoferritin are represented as attractive patches (Figs. 1(b) and 1(d)) in the coarse-grained models. The distance between two patches on each face of the 24-patch model is 0.2σ, where σ is the diameter of the particle. The patches are placed on the longer diagonal, at equal distance from the centroid of the face.

II. MODEL AND SIMULATION METHODS

The attractive interaction between the particles is considered as a square-well potential in combination with an orientation dependent term, f, as

$$U = \begin{cases} \infty, & 0 \le r_{ij} < \sigma \\ -\varepsilon \times f(\Omega_i, \Omega_j), & \sigma \le r_{ij} < \sigma + \xi \end{cases}, \quad (1)$$

where ε and ξ are the strength and range of attraction, and r_{ij} is the center-to-center distance between the particles. The expression for f is chosen to mimic hydrogen-bonding interaction and reads as[12]

$$f(\Omega_i, \Omega_j) = \exp\left(-\frac{\theta_{k,ij}^2}{2\delta^2}\right) \times \exp\left(-\frac{\theta_{l,ji}^2}{2\delta^2}\right) \quad (2)$$

for the 30-patch model, and

$$f(\Omega_i, \Omega_j) = \exp\left(-\frac{(\theta_0 - \theta_{kl,ij})^2}{2\delta^2}\right) \quad (3)$$

for the 24-patch model.

In these expressions, $\theta_{k,ij}$ ($\theta_{l,ji}$) denotes the angle between patch vector $\vec{k}$ of the ith particle (patch vector $\vec{l}$ of the jth particle) which makes the minimum angle with $\vec{r}_{ij}$ ($\vec{r}_{ji}$) and the parameter δ defines the width of a patch. Unlike the 30-patch model where two particles interact only via a single patch on each particle, the 24-patch particles interact via a pair of patches from each particle, as we inferred from the crystallographic data of apoferritin.[10] We use $\theta_0 = 2.72$ rad as the equilibrium angle between patches, when two particles are bonded through a pair of patches. $\theta_{kl,ij}$ denotes the minimum angle between a patch vector $\vec{k}$ of the ith particle and a patch vector $\vec{l}$ of the jth particle.

We perform simulated annealing simulations with either N = 30 or 50 patchy particles in a cubic box of length 7.937σ, using periodic boundary conditions. We define a reduced temperature $\bar{T} = k_B T/\varepsilon$, where k_B is the Boltzmann constant and T the temperature. We use $\xi = 0.05\sigma$ and $\delta = 0.1$ rad for the 30-patch model and $\delta = 0.2$ rad for the 24-patch model. We chose the patch size (δ) such that the transition temperature corresponds to the energy scale of hydrogen bonding ($\sim 5 - 10\ k_B T$). A narrow patch would induce self-assembly at higher attraction strength, while a wide patch would lead to overlap of nearby patches, destroying the point symmetry. However, to demonstrate that the sheet-like assemblies are formed not just for one particular T-δ values, we have explored a range of δ values and obtained the corresponding transition temperatures to show fluid to sheet transition. The phase-diagrams of POM and apoferritin are shown in supplementary material Figs. 1 and 2, respectively.[17]

Random initial configurations are used in the simulation. The simulations were started at high temperature ($\bar{T}_0 = 0.2$, that corresponds to a gas-like configuration of the particles as the patch is very narrow). We then decrease the temperature in steps according to a cooling scheme defined by $\bar{T}_n = \alpha^n \bar{T}_0$, where α is chosen in the range of 0.97 to 0.99. At each step, the system is equilibrated over 20–30 million Monte

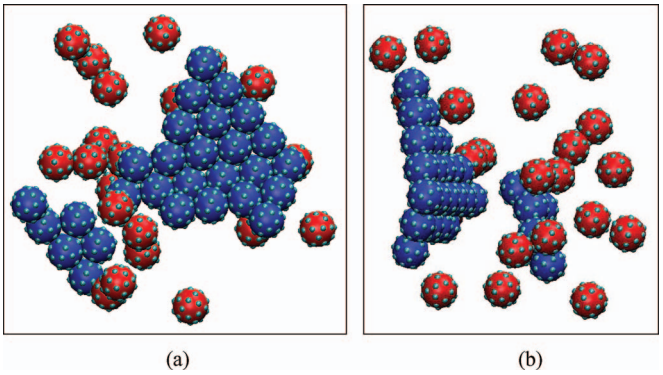

FIG. 2. (a) Single-layered sheet-like assembly obtained at a temperature $\bar{T} = 0.112$ from the 30-patch particles. (b) Side-view of (a) showing single-layer structure. The particles that are in the sheets are highlighted in blue color.

Carlo (MC) cycles. Each MC cycle consists of a translational and rotational move (using the quaternion representation[13]) per particle. The maximum values for the displacement and degree of rotation for the trial moves are adjusted to maintain 40–60% acceptance. The transition temperature is identified as the temperature at which there is a sharp decrease in potential energy, or a peak in the heat capacity versus temperature curve. After obtaining the transition temperature, we perform conventional Monte Carlo simulations at the transition temperature.

III. RESULTS AND DISCUSSION

Figure 2(a) shows a representative snapshot obtained from simulation of 30-patch particles at $\tilde{T}_0 = 0.112$, corresponding to an attraction strength of $\varepsilon = 8.9k_BT$, and Fig. 2(b) shows the side view. We observe that the 30-patch particles spontaneously self-assemble into a sheet-like structure. It is surprising that the spherical particles intrinsically stabilize a two-dimensional crystal, although the patches are distributed in three dimensions. We find that more than 50% of the particles self-assemble into a sheet-like structure with hexagonal close packing, and the remaining particles exist in the form of a gas of monomers, dimmers, trimers at the chosen density. Adding a screened-Coulombic interaction to the pair potential in Eq. (1) in combination with deceasing the temperature increases the fraction of particles in sheets significantly, as will be discussed later.

Why is the formation of a two-dimensional crystal preferred in the 30-patch model? At low volume fractions, the cluster grows by successive addition of individual particles. If we consider the early stage of growth, starting with a dimer forming a single bond, there are three ways of binding a third particle and forming a trimer: perpendicular to the C2 (Fig. 3(a)), C3 (Fig. 3(b)), and C5 axes (Fig. 3(c)). In the first two situations, there are 3 bonds per trimer compared to two bonds in the last possibility. One would then expect the trimer perpendicular to C2 axis to be more stable than the other because removing a particle from the trimer requires breaking of two bonds, which is highly improbable due to 18 k_BT (2 times the bond energy) of dissociation energy. In contrast, the trimer perpendicular to C5 axis is often destabilized because removing a particle requires breaking of only one bond. A new particle is likely to add to the trimer such that it maximizes the number of bonds it can make. This preference seems to occur in the plane perpendicular to the C2 axis because it offers either 2 or 3 bonds for the new particle. If the new particle adds to the top or bottom of the trimer, then it makes only one bond, which can easily be broken. This means that, although there are six sites for 3D and three sites for 2D growth, a new particle makes more bonds at a 2D site compared to a 3D site, leading to the stabilization of a sheet-like structure. Therefore, the fate of the cluster structure is determined by the structure of the initial trimer.

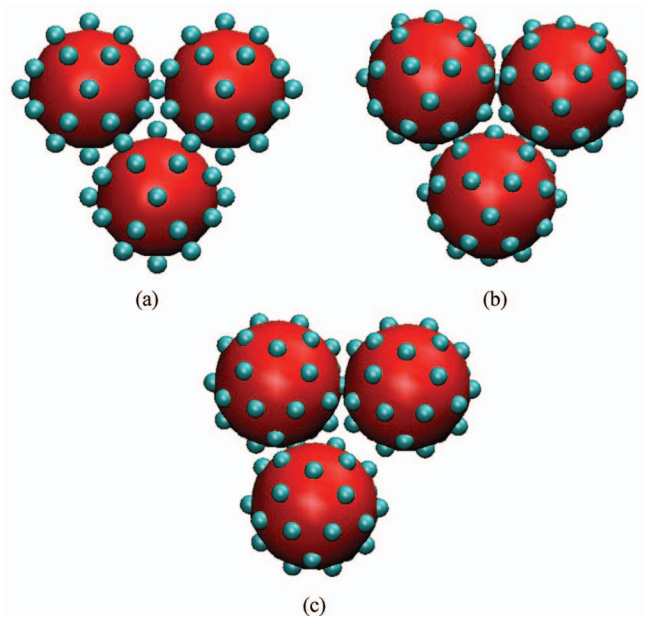

FIG. 3. Trimers of 30-patch model perpendicular to (a) C2, (b) C3, and (c) C5 symmetry axes. Note that there are 3 bonds both in (a) and (b), and 2 bonds in (c).

The crystal structure dictated by patch symmetry is compatible to the experimentally observed rhombohedral structure,[9] which consists of a stack of planes perpendicular to a C2 axis of symmetry. From a bond-energy point of view, for the bond energies considered here (i.e., at least several k_BT), a 3D crystal would be preferred as each particle can make 8 bonds in the crystal. However, as a consequence of the anisotropy in number of bonds in different planes of the crystal, the sheet-like structure with the maximum number of bonds per particle (6) is observed as a metastable structure. The stability of sheet-like structures implies that the crystal may form by stacking of sheets, although this process is expected to be extremely slow because two or more such sheets should come together with proper orientation.

It was reported that the POMs should carry a few charges to stabilize the shells.[4] Repulsive interactions may help stabilize sheet-like structures in two ways. Firstly, particles at the edges of the sheets experience less repulsion than on the top of the sheets, which favors the lateral growth of the sheets. We verified this effect by incorporating repulsive (isotropic) interactions of the type $Ae^{-\kappa r_{ij}}/r_{ij}$, where A is a parameter related to the surface potential,[14] and κ is the inverse Debye screening length. If repulsive interactions are included ($A = 0.5k_BT\sigma$, $\kappa^{-1} = 2\sigma$; A corresponds to a surface potential value of 0.6 k_BT), the fraction of patchy particles within the sheet is more than 80%, which is significantly higher than without repulsive interactions. A snapshot of self-assembled structure under this condition and its side-view are shown in Figs. 4(a) and 4(b).

Secondly, repulsive interactions between the sheets prolong the stacking process to form the crystal phase. Meanwhile the sheets have enough time to fold to form a hollow shell. Folding is energetically favored, at least compared to a sheet, as it minimizes the number of dangling bonds along the edges. This argument is supported by the fact that the timescale of the formation of a shell ranges from few weeks to months.[15] The fragments of sheets can coalesce and grow to a critical size, which is determined by the number of

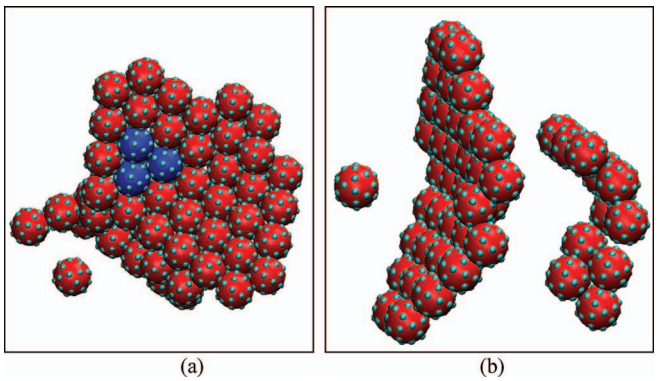

FIG. 4. (a) Single-layered sheet-like assembly obtained at a temperature $\bar{T} = 0.104$ when repulsive interactions are included ($A = 0.5k_BT\sigma$, $\kappa^{-1} = 2\sigma$) in the 30-patch particles. The trimer (C2 symmetric) highlighted in blue shows how the nucleus (FIG. 3(a)) fits in with the sheet-like structure. (b) Side-view of (a) showing single-layer structure.

unsaturated bonds along the edges and the electrostatic energy.[16] Once a critical size of the sheet is reached (~1000 particles), the sheets are potentially eligible to fold into shells due to large fluctuations. We have shown here that sheet-like structures in Keplerate-type POMs are kinetically stabilized due to their preferred growth in 2D, as dictated by the icosahedral point symmetry of their patches.

We now turn to the 24-patch model for apoferritin. Figure 5(a) shows a representative snapshot of the self- assembly of 24-patch particles obtained from one of the simulations performed at $\bar{T} = 0.145$, corresponding to an attraction strength of $\varepsilon = 8.9k_BT$. We predominantly observe particles assembled in small planar structures with hexagonal packing (111 plane) in addition to few 3D-like crystal clusters. Figure 5(b) shows the arrangement of atoms in the ⟨111⟩ plane of a FCC crystal to compare with the structure shown in Fig. 5(a). The stability of 2D structures appears to be attributed to both kinetic growth mechanism and entropic reasons. In the early stage of growth, after a trimer is formed, the fourth particle is more likely to be attached along the plane of the trimer as it has 3 binding sites, compared to only one site for the 3D like structure (see Fig. 5(c)). Because 4 bonds are formed in the 2D binding sites, it is extremely unlikely that these spontaneously break at $\bar{T} = 0.145$. This leads to the abundance of 2D structures. At even lower temperature this effect should be even more significant.

We tested this by running many independent simulations (~30) at two temperatures ($\bar{T} = 0.145$ and 0.1), where we fixed a trimer at the center of the box and randomly introduced a test particle in the box and observed where it ended up. For $\bar{T} = 0.145$, we found that 41% form 2D and 33% form 3D structures with three new bonds, while the remaining particles form 3D aggregates with only two bonds and monomer. For $\bar{T} = 0.1$, we found 33% 1D, 24% 2D and only 7% 3D structures with three bonds because bonds are irreversible at this temperature. Again, the remaining particles are in the form of 3D aggregates with only two bonds. At low temperatures even 1D structures become stable. Therefore, the metastable structures (2D structures) obtained in the simulations are often governed by the initial growth mechanisms when the degree of reversibility of bonds is low.

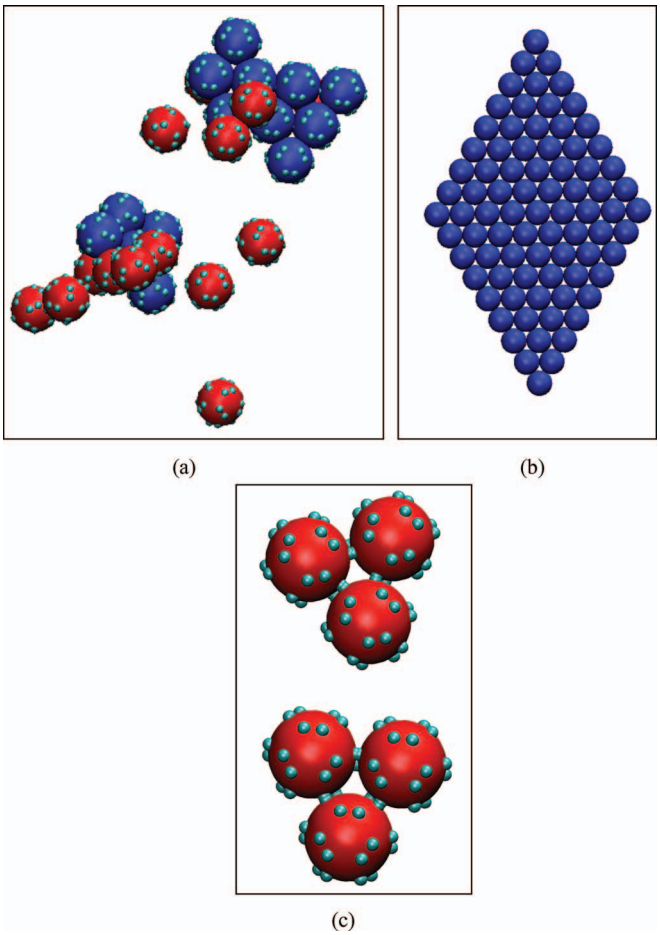

FIG. 5. (a) An assembly of 24-patch model obtained for $\bar{T} = 0.145$, where short ⟨111⟩ planes can be seen as highlighted in blue color. (b) Shows the ⟨111⟩ plane of an FCC crystal for comparison. (c) Top and bottom views of a trimer showing differences in binding symmetry. Only the bottom configuration binds a new particle with 6 bonds (3 pairs). Note that these trimers are found in the assemblies shown in (a).

2D structures are entropically favored. A simple estimate of the configurational entropy of a trimer (42 possibilities for 2D and 8 possibilities for 3D) is $T\Delta S_c = k_B T \ln(42/8) = 1.65\ k_B T$. We also measured the mean square displacement (MSD) of a test particle bonded to a trimer at 2D and 3D positions and estimated the vibrational entropy contribution as $T\Delta S_v = k_B T \ln(MSD_{2D}/MSD_{3D}) = 0.63\ k_B T$. MSD provides a measure of vibrational motion when the test particle is bonded to the trimer. Therefore, 2D structures gain a net entropic contribution of 2.3 $k_B T$. Although this entropic contribution is quite small compared to twice the bond energy differences between 2D and 3D structures, the effect is not negligible. Both these arguments imply that the 24-patch model has a subtle preference to form a two-dimensional crystal that is driven by the growth mechanism and slightly stabilized by entropy.

Sheet-like intermediate structures in the course of crystallization have been reported in experiments, both for POM[15] and apoferritin.[5] POMs are known to form large hollow shell-like structures as intermediates en route to crystallization[15] as mentioned in the Introduction section. It remained paradoxical that spherical POMs stabilize two-dimensional crystals,

which appears at the outset incompatible with their spherical shape. We resolved this issue by implementing patchy and directional attractions. The simulation results suggest a novel route to crystallization in which the sheets can be intermediate structures. Because of the symmetry of the patches, a part of the crystal (sheet/plane) is formed via self-assembly of monomers. These sheets are likely to stack up to build the crystal compatible to the symmetry of the patches. Our hypothesis for the crystallization of patchy particles is consistent with the observation of two-layered POM shells formed over very long timescales.[15]

Apoferritin is known to grow layer-by-layer onto the crystal surface,[5] similar to the layered structure (111 plane) observed in the simulations. However, in experiments studying nucleation of apoferritin using atomic force microscopy (AFM), it was found that apoferritin self-assembles as short planer objects along the 110 plane and subsequently grow layer-by-layer to form a FCC crystal.[5] However, in our simulations we observe assemblies consisting of 111 planes instead of 110 planes. The preference to form 110 plane yet remains puzzling. Although we do not exactly explain the structure of the clusters obtained in experiments on apoferritin, with the level of coarse-graining considered, we are able to establish that even spherical patchy particle with cubic point symmetric patches could stabilize two-dimensional crystals.

IV. CONCLUSIONS

We have showed that two-dimensional crystals such as sheets could be stabilized by spherical patchy particles, even if the sticky patches are distributed all over the surface of the particle. Besides that our finding explains the observation of hollow shell-like structures in POMs and layered growth of apoferritin, it may also have important consequences in nucleation and growth of patchy colloids, proteins, inorganic molecules and nanocrystals, where the critical nucleus could be non-spherical.

[1] A. Patti and M. Dijkstra, Phys. Rev. Lett. **102**, 128301 (2009).
[2] J. Israelachvili, *Intermolecular and Surface Forces* (Academic, San Diego, CA, 1992).
[3] Z. Tang, Z. Zhang, Y. Wang, S. C. Glotzer, and N. Kotov, Science **314**, 274 (2006).
[4] T. Liu *et al.*, J. Am. Chem. Soc. **128**, 15914 (2006).
[5] S.-T. Yau and P. G. Vekilov, Nature (London) **406**, 494 (2000).
[6] A. Muller, Nat. Chem. **1**, 13 (2009).
[7] Z. Zhang and S. C. Glotzer, Nano Lett. **4**, 1407 (2004).
[8] T. Liu *et al.*, Nature **426**, 59 (2003).
[9] A. Muller *et al.*, Angew. Chem. Int. Ed. **38**, 3238 (1999).
[10] P. D. Hempstead *et al.*, J. Mol. Biol. **268**, 424 (1997).
[11] Analysis of the crystallographic data of POM $\{Mo_{72\times 30}; X = Fe^{3+}\}$ (from Cambridge Crystallographic Data Centre No – 132027) reveals that the distance between the oxygen atoms of the water molecules bound to the linker molecules between two neighbouring POMs lies in the range of 2.7 – 2.9 A, which implies hydrogen bonding interactions.
[12] E. G. Noya, C. Vega, J. P. K. Doye, and A. A. Louis, J. Chem. Phys. **127**, 054501 (2007).
[13] M. P. Allen and D. J. Tildesley, *Computer Simulation of Liquids* (Oxford University Press, New York, 1987).
[14] E. Mani, E. Sanz, P. G. Bolhuis, and W. K. Kegel, J. Phys. Chem. C **114**, 7780 (2010).
[15] S. J. Veen *et al.*, (To be submitted).
[16] A. A. Verhoeff *et al.*, Phys. Rev. Lett. **99**, 066104 (2007).
[17] See supplementary material at http://dx.doi.org/10.1063/1.3702203 for the phase diagrams of patchy particles (SM Figs. 1 and 2).